Eur. J. Biochem. **270**, 137–145 (2003) © FEBS 2003 doi:10.1046/j.1432-1033.2003.03373.x

Molecular characterization of artemin and ferritin from *Artemia franciscana*

Tao Chen[1,*], Reinout Amons[2], James S. Clegg[3], Alden H. Warner[4] and Thomas H. MacRae[1]

[1]*Department of Biology, Dalhousie University, Halifax, Nova Scotia, Canada;* [2]*Department of Molecular Cell Biology, Sylvius Laboratory, Leiden, the Netherlands;* [3]*Section of Molecular and Cellular Biology, University of California, Davis, Bodega Bay, CA, USA;* [4]*Department of Biological Sciences, University of Windsor, Windsor, Ontario, Canada*

Embryos of the brine shrimp, *Artemia franciscana*, exhibit remarkable resistance to physiological stress, which is temporally correlated with the presence of two proteins, one a small heat shock/α-crystallin protein termed p26 and the other called artemin, of unknown function. Artemin was sequenced previously by Edman degradation, and its relationship to ferritin, an iron storage protein, established. The isolation from an *Artemia* expressed sequence tag library of artemin and ferritin cDNAs extends this work. Artemin cDNA was found to contain an ORF of 693 nucleotides, and its deduced amino-acid sequence, except for the initiator methionine, was identical with that determined previously. Ferritin cDNA is 725 bp in length with an ORF of 516 nucleotides. Artemin amino-acid residues 32–185 are most similar to ferritin, but artemin is enriched in cysteines. The abundance of cysteines and their intramolecular spatial distribution suggest that artemin protects embryos against oxidative damage and/or that its function is redox regulated. The conserved regions in artemin and ferritin monomers are structurally similar to one another and both proteins assemble into oligomers. However, modeling of the quaternary structure indicated that artemin multimers lack the central space used for metal storage that characterizes ferritin oligomers, implying different roles for this protein. Probing of Northern blots revealed two artemin transcripts, one of 3.5 kb and another of 2.2 kb. These transcripts decreased in parallel and had almost disappeared by 16 h of development. The ferritin transcript of 0.8 kb increased slightly during reinitiation of development, then declined, and was almost completely gone by 16 h. Clearly, the loss of artemin and ferritin during embryo development is due to transcriptional regulation and proteolytic degradation of the proteins.

Keywords: *Artemia franciscana*; artemin; development; ferritin; protein structure.

The brine shrimp, *Artemia franciscana*, exhibits an unusual life history in which embryos either develop ovoviviparously, leading to release of swimming larvae from females, or development is interrupted and embryos are discharged as encysted gastrulae (cysts), a sequence of events termed oviparous development [1]. Cysts enter diapause which is characterized by profoundly reduced metabolic activity [2,3]. Encysted embryos, either in diapause or after the condition is terminated, are extremely resistant to stress [4–7], a characteristic thought to be partly dependent upon p26, a small heat shock/α-crystallin protein [8–14]. The small heat shock/α-crystallin proteins are molecular chaperones which prevent irreversible denaturation of proteins, thereby exhibiting an important function within stressed cells [15,16]. Proteins other than p26 are abundant in cysts, and one of these, artemin, is described in this paper. The term artemin was first used by Slobin [17] to refer to this protein in *Artemia*, but was used much later to designate a member of the glial cell line-derived neurotrophic factor (GDNF) family [18]. In addition, other work revealed the presence of a protein complex in *Artemia* termed the 19S complex [19–21]. Although there was initially some disagreement, it was recognized that the protein was the same as artemin, and that terminology is used in this paper.

Artemin is a major protein of encysted *Artemia* embryos, comprising about 12% of the soluble cellular protein, but it is almost completely absent from nauplius larvae [17,19,22]. As determined by Edman degradation, artemin monomers consist of 229 amino-acid residues and exhibit a molecular mass of 25 976 Da. Artemin and ferritin have comparable primary structures, although artemin is 45–50 residues longer than most ferritins, and they form oligomers of similar size [23]. Thus, purified artemin has a sedimentation constant of 19S and a molecular mass of 573–610 kDa, probably consisting of 24 subunits. It was suggested that the subunits are linked by intermolecular disulfide bridges [19–21]. Electron microscopic examination of artemin revealed a monodisperse complex with a rosette-like appearance [23].

Vertebrate ferritins are about 180 amino-acid residues in length and composed in various ratios of two highly conserved subunits, H and L [24–27]. Multiple H and L

Correspondence to T. H. MacRae, Department of Biology, Dalhousie University, Halifax, N.S., B3H 4J1, Canada.
Fax: 902 494 3736, Tel.: 902 494 6525,
E-mail: tmacrae@is.dal.ca

Abbreviation: EST, expressed sequence tag.

**Present address*: Animal Science and Technology College, Hunan Agricultural University, Changsha, Hunan, People's Republic of China, 410128.

Note: a web page is available at http://is.dal.ca/~biology2/index.html

(Received 9 September 2002, revised 28 October 2002, accepted 18 November 2002)

ferritins, two of which are secreted from cells, are described for *Drosophila* [28,29], and the occurrence of both ferritin types in invertebrates may be the norm. Plants, on the other hand, are thought to contain a single class of ferritin, restricted to plastids and sharing properties of both H and L polypeptides [26,27,30,31]. The 3D structures of several ferritins have been elucidated by X-ray crystallography. Horse L-apoferritin, thought to be representative of the ferritins, consists of large, bundled, parallel helices, termed A, B, C, and D, in addition to a smaller helix, E, at a 60° angle to the helix bundle axis [24–27]. Helices A and B are antiparallel, as are C and D, and they are connected by small loops. A large loop, designated L, connects A and B helices with C and D helices, and L loops of neighboring monomers establish an antiparallel β-sheet, key to ferritin dimer formation. Ferritin monomers assemble into oligomers consisting of 24 subunits arranged in 4-3-2 symmetry and producing a hollow sphere. Fourfold channels in the shell of the sphere are lined by the hydrophobic sides of four E helices from different subunits. Eight hydrophilic channels constructed with acidic residues from the D helices of three neighboring subunits also occur in the multimer shell, and these have wide, funnel-like structures composed of exterior residues. The central cavity of the ferritin oligomer is ≈ 8 nm in diameter and houses up to 4500 Fe(III) atoms as an inorganic complex called ferrihydrite. Ferritins have low cysteine content in spite of their substantial ability to bind metals, and only Cys126, numbered according to horse L-ferritin, is conserved in vertebrate species. Ferritins are very resistant to denaturation by heat and chemicals such as urea and guanidinium chloride [24], and the degradation of ferritin *in vivo* is inhibited by excess iron [32].

To address questions of structure and function, artemin and ferritin cDNAs obtained from an *Artemia* expressed sequence tag (EST) library (unpublished work), were characterized. The artemin amino-acid sequence deduced from the cloned cDNA was identical with that derived earlier by Edman degradation, and it was similar to the primary structure of *Artemia* ferritin, determined for the first time in this study. Computer modeling revealed that the 3D structures of ferritins from *Artemia* and other organisms are comparable, and that monomers of artemin and ferritin may be organized similarly in their respective multimers. However, the increased length of artemin and the spatial disposition of its C-terminal tail upon oligomerization support electron microscopic observations that artemin multimers lack hollow centers [20,23]. Thus, even though artemin and ferritin exhibit similar structure and temporal expression, they are almost certain to perform different functions during *Artemia* development. In addition, analyses of ferritin and artemin mRNA suggest that expression of the genes for both proteins is developmentally regulated in *Artemia*.

Experimental procedures

Incubation of *Artemia*

Encysted *Artemia* embryos (cysts) from Sanders Brine Shrimp Co., Ogden, UT, USA were hydrated in distilled water at 4 °C for 6 h. Cysts that sank were collected by suction on a Buchner funnel, rinsed several times with cold distilled water, and incubated at 27 °C in hatch medium with shaking at 200 r.p.m. [33]. *Artemia* collected after 0, 8 and 10 h of development were encysted. Emerged embryos, termed E2, were harvested after 13 h of incubation, and newly hatched larvae (nauplii) were obtained after 16 h of development [34–36].

Preparation of *Artemia* cDNA and EST libraries

Artemia libraries were constructed using mRNA prepared from 1 g emerged larvae homogenized in 2 mL TRIZOL reagent (Gibco-BRL) at room temperature. Homogenized samples were incubated at room temperature for 5 min, and 0.4 mL chloroform was added, followed by vigorous shaking and incubation at room temperature for 15 min. RNA was precipitated from the aqueous phase by adding 1.0 mL propan-2-ol, incubating at room temperature for 10 min and centrifuging at 12 000 ***g*** for 10 min. Supernatants were discarded and pellets washed by vortex mixing in 2 mL 75% ethanol, collected by centrifugation at 7500 ***g*** for 10 min, air-dried for 20 min, dissolved in diethyl pyrocarbonate-treated water and stored at −70 °C. Poly(A)-rich mRNA was obtained by use of an mRNA purification kit (Pharmacia Biotech). cDNA was generated with a synthesis kit (Stratagene) using random nonamers and oligo(dT) primers with an *Xho*I restriction site added to the 5′ end of the oligo(dT) primer. *Eco*RI adapters were added to both ends of the cDNA, which was digested with *Xho*I, inserted into *Eco*RI–*Xho*I-digested Uni-Zap XR, and packaged in λ phage using the ZAP-cDNA Gigapack III Gold Cloning Kit (Stratagene). The λ phage library was converted into pBluescript plasmids by *in vivo* mass excision according to the manufacturer's instructions (Stratagene).

To prepare an *Artemia* EST library, individual cDNA clones were selected randomly from the converted library, and template DNA was recovered from bacterial lysates [37]. The DNA was sequenced with an AB1373 automated sequencer and the AmpliTaqFS dye terminator cycle sequencing ready reaction kit (Perkin-Elmer). Sequence information was obtained by a single pass from each selected clone using a T3 primer at the 5′ end and DNA Strider 1.2 for analysis [38].

Structural characterization of artemin and ferritin cDNAs and proteins

Of the 672 analyzed clones in the *Artemia* EST library, one artemin and two identical ferritin cDNAs were identified upon single-pass sequencing. Plasmid DNA was isolated from the artemin and ferritin clones using a plasmid extraction kit (Qiagen) and sequenced on two separate occasions from both the 3′ and 5′ directions using T3 and T7 primers. Amino-acid sequences were deduced from nucleotide sequences, and alignments were performed using CLUSTALW at http://www2.ebi.ac.uk/clustalw/. Secondary structures of artemin and ferritin were analyzed using Protein Predict available at http://cubic.bioc.columbia.edu/predictprotein/and helical wheel presentation available at http://cti.itc.virginia.edu/~cmg/Demo/wheel/wheelApp.html. 3D structure was predicted using the computer program Cn3D available at the NCBI web site.

Phylogenetic analysis

To examine evolutionary relationships, a phylogenetic tree was constructed by comparing protein sequences deduced in this study for artemin and *Artemia* ferritin with selected animal ferritins archived in databases and listed in the figure legend. The protein sequences were initially aligned with CLUSTALX, after which the distances between proteins were calculated using Poisson correction and the tree inferred by the NJ method. The latter two steps were carried out with TREECON for Windows authored by Yves van de Peer, University of Antwerp (UIA) in 1994 and 1998. Bootstrap values over 75 are shown, and the tree was rooted with less complex animals as the outgroup.

Northern-blotting

mRNA was prepared after incubations of 0, 8, 10, 13 and 16 h by homogenizing 200 mg wet weight *Artemia* at each developmental stage. Then 25 μg total RNA from each sample was electrophoresed in formaldehyde/agarose gels at 3 $V \cdot cm^{-1}$ for 2.5 h, transferred to nylon membranes, and immobilized by UV cross-linking for 1 min. The Northern blots were probed with an artemin cDNA fragment that encompassed nucleotides 530–830, encoding residues 169–230 of the ORF and flanked by 112 bp of the 3′-UTR. The ferritin probe took in nucleotides 81–380 of the cloned cDNA, corresponding to residues 3–102 of the ferritin ORF. The probes were labelled by use of the PCR DIG Probe Synthesis Kit (Roche Molecular Biochemicals) using the primers (artemin: 5′-ACCTACACTGCATCGGTTCA-3′, 5′-TCCAACTTGGACGGGCAAC-3′) and (ferritin: 5′-CTTTCACGCTGCAGACAGAA-3′, 5′-GAGAGCGTC TTCCATGGCT-3′). Blots were prehybridized in DIG-Easy Hyb (Roche Molecular Biochemicals) at 50 °C for 30 min, then hybridized overnight to labeled probes at the same temperature before being washed once with 2 × NaCl/Cit containing 0.1% SDS for 5 min at room temperature with shaking, and twice with 0.1 × NaCl/Cit containing 0.1% SDS for 15 min at 68 °C. The membranes were then washed with washing buffer [0.1 M maleic acid, 0.15 M NaCl, 0.3%

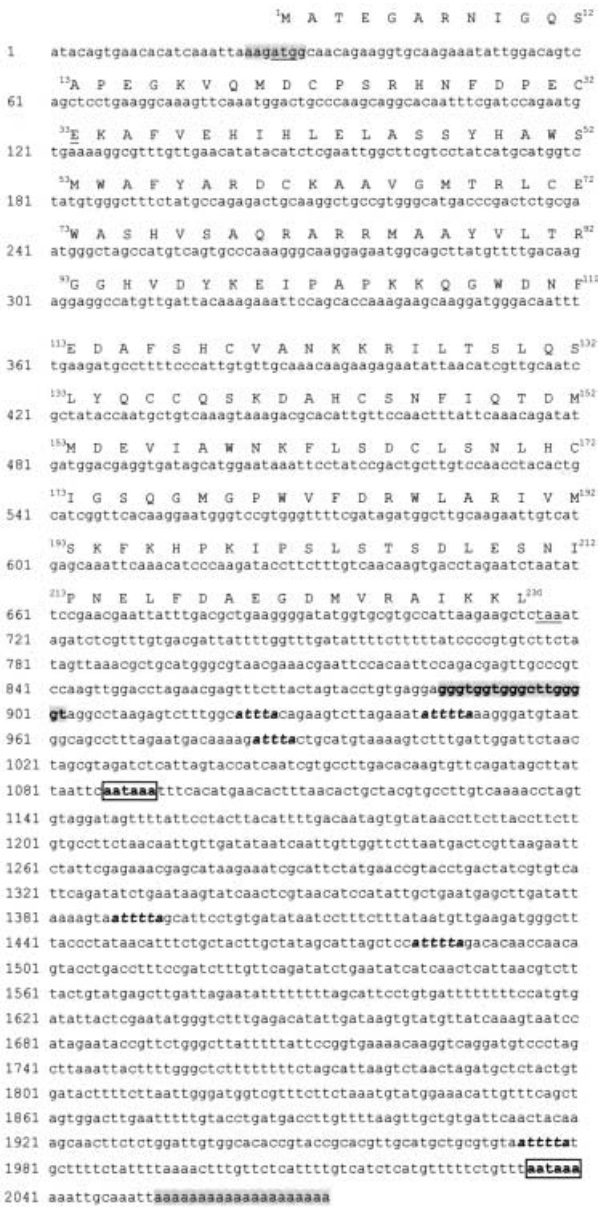

Fig. 1. Nucleotide and amino-acid sequences of artemin. The nucleotide sequence of artemin cDNA was determined as described in Experimental Procedures, and from this the amino-acid sequence was deduced. The initiation (ATG) and termination (TAA) codons are underlined. The ribosome binding site (AAGATGG) and the poly(A) tail are shaded grey. The polyadenylation signals, AATAAA, are in bold and boxed, the ATTTA sequence and its variant ATTTTA are in bold and italicized, and a G/T stretch is in bold and shaded grey.

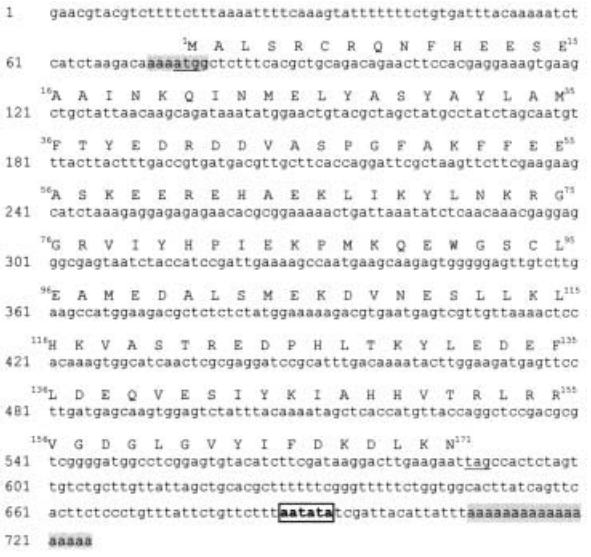

Fig. 2. Nucleotide and amino-acid sequences of *Artemia* ferritin. The nucleotide sequence of *Artemia* ferritin cDNA was determined as described in Experimental Procedures, and from this the amino-acid sequence was deduced. The initiation (ATG) and termination (TAG) codons are underlined, and the poly(A) tail is shaded grey. The polyadenylation signal AATATA is in bold and boxed, while the initiation codon is embedded in the shaded sequence, AAAATGG, a typical ribosome binding site.

(v/v) Tween 20, pH 7.5] at room temperature and incubated with shaking in freshly prepared blocking buffer for 30 min. Then 20 ml antibody solution consisting of antidigoxigenin-alkaline phosphatase and blocking buffer at a ratio of 1 : 10 000 was added, the blot was incubated at room temperature, washed twice with washing buffer, allowed to react with CDP-Star, and exposed to RX-B Blue autoradiography film (Labscientific Inc.).

Results

Cloning of artemin and ferritin cDNAs

The *Artemia* EST library yielded a single artemin and two identical ferritin cDNAs, for which the corresponding amino-acid sequences were deduced. The artemin cDNA of 2072 bp (accession number AY062896) contained an ORF of 690 bp flanked by a 25-bp 5′-UTR and a 3′-UTR of 1357 bp including a stop codon and poly(A) tail (Fig. 1). The 5′ start codon begins at nucleotide 26 and the stop codon at nucleotide 716. The AUG initiation codon is embedded in the sequence, AAGATGG, a typical eukaryotic ribosome binding sequence of Pu-X-X-AUGG. Two polyadenylation signals of AATAAA are located within the 3′-UTR at nucleotides 1087–1092 and 2035–40, respectively. A GT box of 18 consecutive nucleotides required for efficient processing and polyadenylation of mRNA appears at position 885–902. A poly(A) tail of 20 bp is located at the end of the 3′-UTR, demonstrating that most, if not all, of the artemin cDNA was cloned. The artemin 3′-UTR has a high AT percentage, with 28.4% A, 37.1% T, 17.2% G and 17.3% C. The deduced amino-acid sequence of the artemin monomer consists of 230 residues with a calculated molecular mass of 25 976 Da.

The ferritin cDNA (accession number AY062897) of 725 bp consists of an ORF of 516 bp, a 74-bp 5′-UTR and a 138-bp 3′-UTR containing an 18-bp poly(A) tail (Fig. 2). The initiator codon begins at nucleotide 75 and the stop codon at nucleotide 588. The AUG start codon resides in the sequence AAAATGG, and, in contrast with artemin, there is only one polyadenylation signal of AATATA, consisting of nucleotides 687–692. The base compositions, respectively, of the full-length ferritin ORF and its 3′-UTR are 31.2% A, 28.7% T, 19.2% C, 20.9% G and 15.4% A, 47.9% T, 21.3% C, 15.4% G.

Structural comparison of artemin and ferritin

Alignment of amino-acid sequences revealed a limited but clear similarity between representative ferritins and artemin, indicating that they are members of the same protein superfamily (Fig. 3A). *Artemia* ferritin contains residues that constitute a di-iron ferroxidase center (represented in red), thereby aligning it with the H-series of ferritins. Equivalent residues are found at only two sites of the

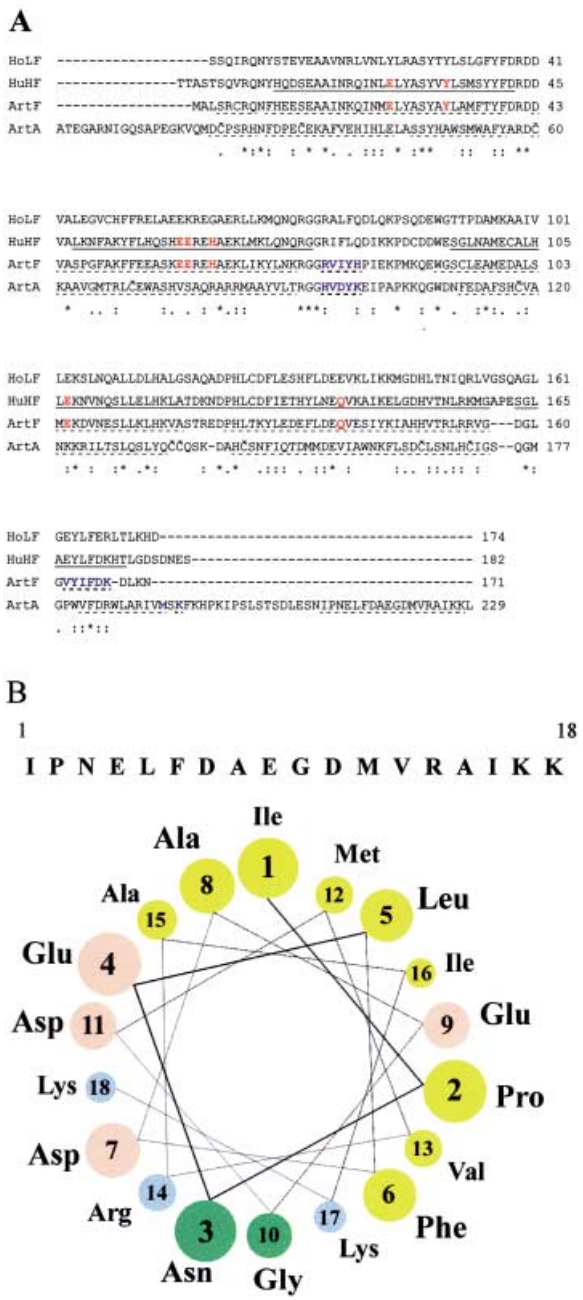

Fig. 3. Sequence alignment of artemin with ferritins and proposed secondary structures. (A) The deduced amino-acid sequences of horse ferritin L (accession number P02791), human ferritin H (accession number P02794), *Artemia* ferritin and artemin were aligned by CLUSTAL W. Solid underlining of human H ferritin sequence represents helical regions found by X-ray analysis. Broken underlining indicates helical regions, and residues in blue indicate β structures in *Artemia* ferritin and artemin. Residues in the di-iron ferroxidase centers of human ferritin H chain and in *Artemia* ferritin are in red. Cysteine residues in the conserved region of artemin are indicated by Č. *, identical or conserved residue in all sequences; :, conserved substitution; ., semiconserved substitution. HoLF, horse ferritin L; HuHF, human ferritin H; ArtF, *Artemia* ferritin; ArtA, artemin. (B) Residues 211–228 of artemin were predicted to form an α-helix when submitted into the program Protein Predict available at http://cubic.bioc.columbia.edu/predictprotein/. The helical wheel presentation was performed with http://cti.itc.virginia.edu/~cmg/Demo/wheel/wheelApp.html. Amino-acid properties are indicated by color: yellow, nonpolar; green, polar; pink, acidic; blue, basic.

artemin sequence, an important difference between the proteins. In contrast with the internal conserved region of the protein, neither the N-terminus nor C-terminus of artemin has similarity to any known protein. Protein Predict indicates a secondary structure for *Artemia* ferritin and artemin that is similar to the overlapping regions of ferritins from other organisms (Fig. 3A). No distinctive secondary structure was shown by computer modeling for the N-terminal extension of artemin. In contrast, residues 211–228 of the C-terminus are predicted to form a helix (Fig. 3B). The helix is amphipathic, and the hydrophilic side features an asymmetric charge distribution, being predominately basic in its C-terminus and acidic in the N-terminus.

From predictions of secondary structure similarities, the tertiary structures of *Artemia* ferritin and artemin are expected to be the same as for other eukaryotic ferritins. In support of this proposal, 3D structure predictions revealed that the tertiary structure of the artemin monomer, with the exception of its amino and carboxy domains, was the same as the tertiary structure of human H ferritin (Fig. 4). One intriguing aspect of artemin revealed by the analysis of tertiary structure is that constituent cysteines cluster mainly at the ends of helices, localized in regions of close proximity, and are therefore potentially able to form disulfide bridges (Fig. 4). In addition, given the similarities between primary, secondary and tertiary structures, it is reasonable to expect that artemin and the ferritins have related quaternary structures. In this context, ferritin monomers are all-helix proteins, with helices A to D arranged as a bundle exhibiting +/– parallel axes, and the structural units of ferritin multimers in higher eukaryotic organisms are dimers of either H-type or L-type ferritin (Fig. 5). The dimers have the same structural elements as their constitutive monomers, and they contain an antiparallel sheet consisting of the L and L′ loops. The two short E helices in the ferritin dimer are separated spatially, but in the multimer four parallel E-helix construct a fourfold

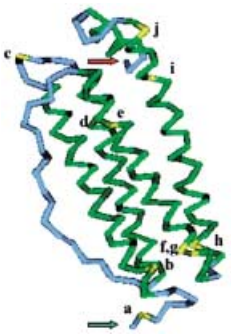

Residue Number	Location in Artemin
C21 (a)	Outside area of homology
C31 (b)	Beginning of helix A
C60 (c)	Loop between helices A and B
C70 (d)	Helix B
C118 (e)	Helix C
C135 (f)	End of helix C
C136 (g)	End of helix C
C143 (h)	Beginning of helix D
C166 (i)	Helix D
C172 (j)	End of helix D

Fig. 4. Human H ferritin and the positioning of cysteine residues in artemin. A monomer of human H ferritin was depicted in Cn3D in the so called 'neighbor style' and used as a template for positioning of cysteine residues in artemin. Helical regions are shown in green and coil regions in blue. The first residue visible in the 3D structure of human H ferritin, T-6, is indicated by the green arrow, the last visible residue, G-177, by a red arrow. The positions a–j indicated in yellow correspond to the cysteine residues in artemin. The inserted table lists the cysteine residues and their approximate locations within the proposed spatial structure of artemin.

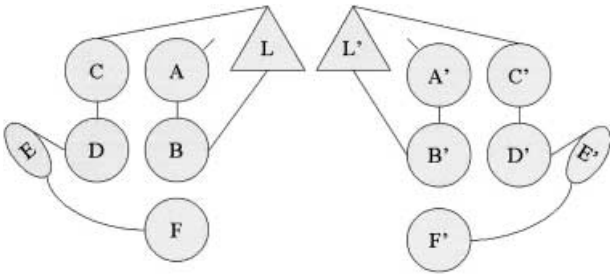

Fig. 5. Schematic representation of an artemin dimer. The figure represents a cut perpendicular to the main axis of an artemin multimer and through the four helix bundles of a dimer. The relationship between two artemin monomers and the orientation of their helical regions within a multimer are visible. Helices AA′, BB′, CC′ and DD′, which also occur in ferritins, and FF′ which are unique to artemin, are represented by circles, and the loops LL′, which form an antiparallel sheet in ferritin, by triangles. The EE′ helices, forming an acute angle with the main helix bundle are indicated by elliptic forms. For the sake of simplicity, we propose that the FF′ helices are +/– parallel to the AA′ to DD′ helices. Covalent connections between the structural elements are indicated by thin lines, and noncovalent interactions are described in the text.

channel fixing four neighboring dimers within the quaternary structure and directing the carboxy ends of the E helices toward the hollow space in apoferritin. Because artemin resembles the basic structure of ferritin, including its twofold symmetry axis, we propose that the artemin E helix and its C-terminal residues are directed toward the multimer center. Moreover, the F helix originating from each monomer has the same orientation as the A to D helices, and the F helices interact with one another (Fig. 5). The latter is feasible because the F helix is amphipathic, its hydrophilic region has an asymmetric charge distribution (Fig. 3B), and the hydrophilic and hydrophobic portions of the F helix are potential candidates for antiparallel helix pairing. For artemin and ferritin multimer structures to be similar under the conditions just described, the artemin F helices are most likely localized within the multimer interior. In agreement with this, the artemin particle is large enough to accommodate the C-terminal regions of all constituent monomers, including the 16 residues of each subunit for which no particular structure was predicted. The unstructured region may fill the space left by the less flexible F helices and, because this stretch of amino-acid residues is hydrophilic, several water molecules may be bound.

Phylogenetic comparisons

Analysis of phylogenetic relationships revealed that the ferritins for those animal species chosen constitute three main subfamilies, one for ferritin H from vertebrates, one for ferritin L from vertebrates, which contains ferritin H from fish and amphibians, and a third for invertebrates in which *Artemia* ferritin and artemin reside (Fig. 6). Artemin and *Artemia* ferritin are most closely related to the *Drosophila* ferritins, with artemin and one of the *Drosophila* ferritins the long branch members of the group.

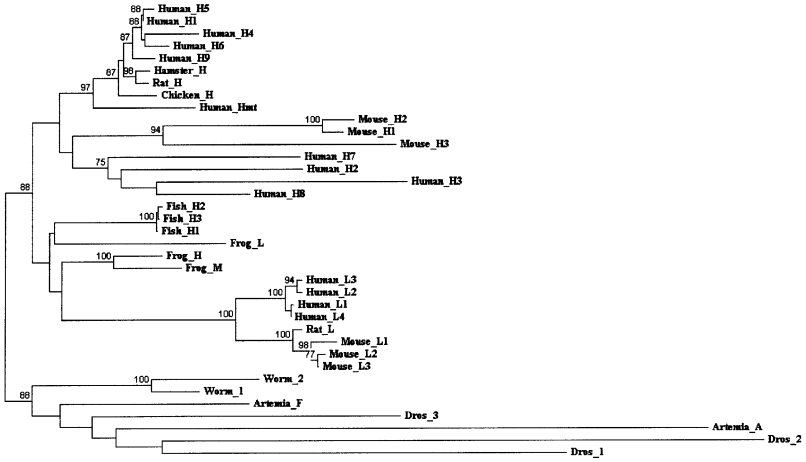

Fig. 6. Phylogenetic comparison of artemin and ferritin. A phylogenetic tree was constructed as described in Experimental Procedures from the deduced amino-acid sequences of artemin, *Artemia* ferritin and ferritins from several other organisms including (accession numbers are in parentheses), Artemia_F, *A. franciscana* ferritin (AAL55398); Artemia_A, *A. franciscana* artemin (AAL55397); Dros_3, *Drosophila melanogaster* CG4349 gene product (AAF48226.1); Dros_1, *D. melanogaster* ferritin (NP_524873); Dros_2, *D. melanogaster* Fer2LCH gene product (AAF57038.1); Fish_H3, *Oncorhynchus mykiss* ferritin H-3 (BBA13148.1); Fish_H2, *O. mykiss* ferritin H-2 (BAA13147.1); Fish_H1, *O. mykiss* ferritin H-1 (BAA13146.1); Frog_M, Bullfrog ferritin chain M (C27805); Frog_L, Bullfrog ferritin chain L (B27805); Frog_H, Bullfrog ferritin chain H (A27805); Worm_1, *Caenorhabditis elegans* hypothetical protein D1037.3 (T33835); Worm_2, *C. elegans* hypothetical protein C54F6.14 (T31870); Chicken_H, Chicken ferritin heavy chain (A26886); Human_H9, *Homo sapiens* apoferritin (CAA25086.1); Human_L4, *H. sapiens* protein for MGC:24401 (AAH16715.1); Human_Hmt, *H. sapiens* mitochondrial ferritin (XP_094231.1); Human_L1, *H. sapiens* ferritin light chain (P02792); Human_L2, *H. sapiens* novel protein similar to ferritin light polypeptide (XP_059268.1); Human_L3, *H. sapiens* novel protein similar to ferritin light polypeptide (CAB43181.1); Human_H1, *H. sapiens* ferritin heavy chain (P02794); Human_H2, *H. sapiens* similar to ferritin heavy polypeptide-like 17 (XP_066582.2); Human_H3, *H. sapiens* similar to ferritin heavy polypeptide 17 (XP_070289.1); Human_H4, *H. sapiens* similar to ferritin H subunit (XP_087282.1); Human_H5, *H. sapiens* ferritin heavy polypeptide 1 (XP_087710.2); Human_H6, *H. sapiens* similar to ferritin heavy subunit (XP_042852.5); Human_H7, *H. sapiens* similar to ferritin H subunit (XP_066695.1); Human_H8, *H. sapiens* ferritin heavy polypeptide-like 17 (AAK31971.1); Rat_L, Rat ferritin light chain (P02793); Rat_H, Rat ferritin heavy chain (P19132); Hamster_H, Hamster ferritin H subunit (P29389); Mouse_H1, *Mus musculus* similar to ferritin heavy polypeptide-like 17 (XP_125269.1); Mouse_H2, *M. musculus* similar to ferritin heavy polypeptide-like 17 (XP_125312.1); Mouse_H3, *M. musculus* similar to ferritin H subunit (XP_142836.1); Mouse_L3, *M. musculus* ferritin light chain (B33355); Mouse_L2, *M. musculus* ferritin light chain 1∼putative (XP_110256.1); Mouse_L1, *M. musculus* ferritin L subunit 1 (XP_135303.1). The bootstrap values are indicated above the lines and the branch length is proportional to the phylogenetic distance (scale bar not shown).

Developmental regulation of artemin and *Artemia* ferritin mRNAs

Probing of Northern blots with a labeled artemin probe revealed bands of ≈ 2.1 and 3.7 kb, the former of expected length based on the size of cloned cDNAs. The mRNA in the upper band of the blot probed with the artemin cDNA remained relatively constant until emergence, and then the transcripts began to disappear, whereas the lower band decreased as development progressed. Neither message was easily detected in hatched nauplii after 16 h of development upon visual inspection of exposed films, but minor traces of mRNA were detected when films were scanned (Figs 7A,C). A single, 0.8-kb band of ferritin mRNA was observed on Northern blots. The ferritin transcript increased slightly during early development and there was a sufficient amount in hatched nauplii to yield a visible band on films (Figs 7B,C).

Discussion

The artemin cDNA encodes a protein identical in sequence, except for the initiator methionine, with that obtained by Edman degradation [37]. Sequence comparisons, achieved without introducing major alignment gaps, revealed similarity between representative ferritins, including a ferritin from *Artemia* characterized in this study, and a stretch of 164 amino-acid residues in artemin; however, the amino and carboxy regions of artemin were extended. Artemin and the ferritins also share secondary structure characteristics, and their spatial arrangement in oligomers is predicted to be the same. That is, the short N-terminal regions of ferritin monomers localize to multimer surfaces, whereas C-termini are directed inwardly and buried in the shell. Thus, on the basis of ferritin structure, the accommodation of artemin N-terminal extensions does not pose spatial constraints because these short, mainly hydrophilic stretches of amino acids protrude from oligomer surfaces into the surrounding medium. The situation for the C-terminus is, however, more complicated because each artemin monomer has 35 extra residues compared with the human ferritin H-chain and 24 of the C-terminal extensions must be packed into each oligomer. Using the Peptide Properties Calculator at http://www.basic.nwu.edu/biotools/proteincalc.html, and a partial specific protein volume of 0.73 $cm^3 \cdot g^{-1}$, the 24 C-terminal artemin extensions in a single oligomer were calculated to occupy ≈ 100 000 $Å^3$. This is about the same volume as the space within the hollow ferritin multimer, which has a

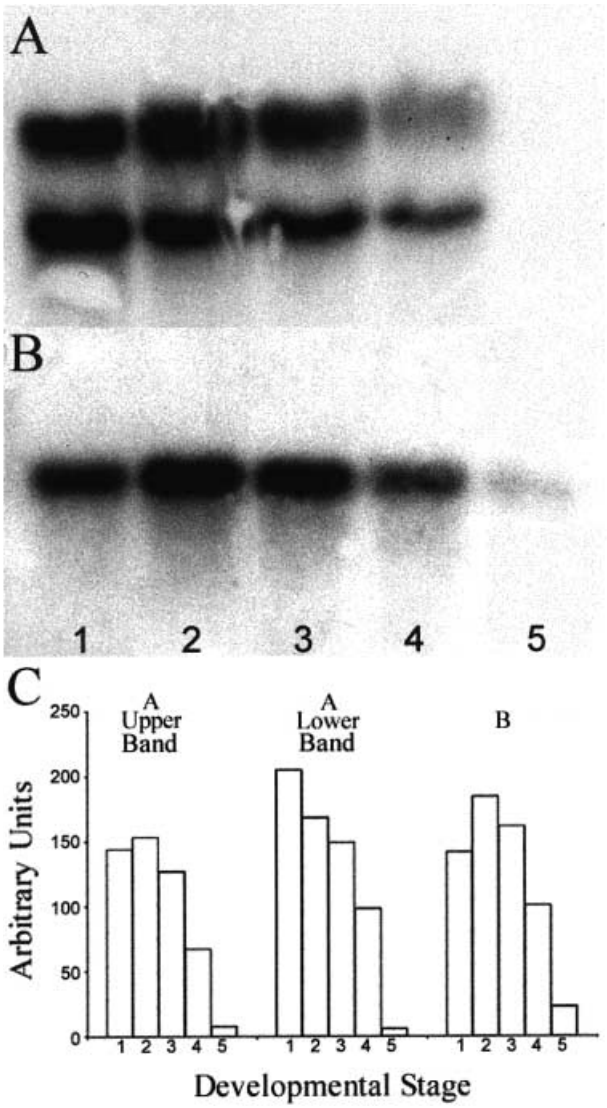

Fig. 7. Developmental regulation of artemin and *Artemia* ferritin mRNAs. Total RNA (25 μg) prepared from *Artemia* after 0, 8, 10, 13, and 16 h of development, lanes 1–5, respectively, was electrophoresed in formaldehyde/agarose gels, blotted to nylon membranes, and hybridized with probes to artemin (A) and ferritin (B). (C) The blots were scanned and the absorbance at each developmental stage was plotted in arbitrary units for the upper and lower bands in (A) and the single band in (B).

diameter of 80 Å [24]. Importantly, examination of purified artemin by electron microscopy does not reveal an obvious central cavity [23]. The simplest interpretation of these observations is that the interior of artemin multimers is filled by the C-terminal extensions of constituent monomers. X-ray analysis revealed that ferritin monomers are sufficiently flexible to allow different H : L ratios in one multimer [27], suggesting that localization of C-terminal extensions within artemin multimers is feasible. This analysis therefore identifies a potential structural difference of functional importance between artemin and ferritin, complementing the observation that biochemically purified artemin lacks metals ([23]; unpublished data). We propose that metals are absent because there is no space in which they can be sequestered.

Artemin and ferritin messages disappear during postdiapause development of *Artemia*, as shown also for the artemin protein [21]. The results indicate that expression of artemin and ferritin genes ceases in encysted embryos, and corresponding mRNAs are degraded as development progresses. The unusually long 3′-UTR of artemin cDNA exhibits AT-rich control elements [39–44]. For example, two ATTTA motifs and four ATTTTA variants occur in the artemin 3′-UTR. These sequences are mRNA stability signals involved in translational regulation through effects on mRNA decay and turnover [41,45–50]. Equally interesting are the two size classes of artemin mRNA, a smaller message that corresponds to the cloned cDNA and a larger transcript of 3.7 kb. That the larger species is an unprocessed artemin mRNA remains a possibility, although preliminary data (not shown) indicate that the artemin gene lacks introns.

Artemin and p26, the latter a small heat shock/α-crystallin protein from *Artemia* with molecular chaperone activity, reside in developing *Artemia* at similar times [8,10,12,13,51]. Artemin may also be a molecular chaperone whose activity, like Hsp33, is redox controlled [52,53]. In support of this proposal, large amounts of artemin, like p26, are present in encysting but not directly developing *Artemia* embryos, and it is not degraded in cysts during long-term anoxia [5]. Thus, artemin may be a stress protein which assumes lesser importance as development progresses, however, chaperone activity has not been demonstrated for this protein. In a parallel study (unpublished data) biochemical analyses indicated that the artemin multimer is thermostable and tightly associated with short, translatable, nonpolyadenylated RNA, suggesting that artemin sequesters selected mRNAs required during oviparous development.

A striking observation is that the conserved sequence of artemin contains nine cysteines, whereas the corresponding region in ferritin has one. Artemin cysteines, with a single exception, cluster at the ends of helices forming two intramolecular regions enriched in these residues, some of which have the potential to form disulfide bridges. The physiological role of artemin, whose cytoplasmic localization is corroborated by the lack of export signal sequences, may depend upon the cysteines and their ability to undergo oxidation/reduction reactions. For example, the cytoplasm of most physiologically normal cells, including those in *Artemia* embryos is reduced, suggesting that artemin is reduced and possesses cysteines rather than cystines. Thus, in addition to acting as a storage site for selected mRNAs, artemin could be a reducing reservoir, shielding cells against oxidation and preventing modification of other proteins, such as tubulin [54]. Although oxidation of proteins could be reversed as quiescent *Artemia* embryos resume development, it is important to protect key proteins required for initiation of growth and differentiation. Protection may be afforded by glutathione and other low molecular mass thiols that visit artemin multimers. In this context, ferritin complexes are thought to 'respire', wherein small compounds such as sugars, chelators and reducing agents enter and exit the multimer interior [24]. As an alternative possibility, the spatial arrangement of cysteines

may constitute a regulatory mechanism, as proposed for human heat shock factor 1 (HSF1), a protein with five cysteines [55]. Oxidation-induced, intramolecular, disulfide cross-linking of HSF1 yields a compact monomer unable to self-associate, and such a post-translational modification inhibits heat-induced transcription *in vivo* which is dependent upon factor trimerization. In another example, activity of the molecular chaperone Hsp33 is controlled by oxidation/reduction, but in contrast with HSF1, disulfide bond formation activates the protein [52,53]. As a final possibility, De Herdt *et al.* [21] suggested that artemin maintains the water content of embryos above a critical level, this based on the finding that artemin has a high hydrodynamic hydration of ≈ 1.25 g H_2O per g protein.

Why ferritin is lost in parallel to artemin is less clear, but may reflect a transient need within encysting embryos for excess capacity to store metals, either as a protective mechanism [32] or in preparation for resumption of development. In the latter context, amplifying the amount of free intracellular iron by lowering the available ferritin to which it can bind enhances cell growth mediated by H-ras [56]. Thus, increasing available intracellular iron by decreasing ferritin in *Artemia* cysts has the potential to promote development if embryo growth had been stalled by ferritin-mediated chelation of iron during early stages of oviparous development.

Acknowledgements

The authors thank Dr Ping Liang for guidance with the phylogenetic analysis, Dr Mike Reith for assistance in construction of the *Artemia* EST library, and Dr Herman Slegers for critical review of the manuscript before submission. The work was supported by a Natural Sciences and Engineering Research Council of Canada Research Grant and a Nova Scotia Health Research Foundation New Opportunity Grant to T.H.M., and in part, by grant MCB-98 07762 from the United States National Science Foundation to J. S. C. T. C. was supported by a grant from the China Scholarship Committee.

References

1. Abatzopoulos, Th.J., Beardmore, J.A., Clegg, J.S. & Sorgeloos, P. (2002) *Artemia: Basic and Applied Biology*. Kluwer Academic Publishers, Dordrecht.
2. MacRae, T.H. (2001) Do stress proteins protect embryos during metabolic arrest and diapause? *Molecular Mechanisms of Metabolic Arrest. Life in Limbo* (Story, K.B., ed.), pp. 169–186. BIOS Scientific Publishers Ltd, Oxford.
3. Clegg, J.S. & Jackson, S.A. (1998) The metabolic status of quiescent and diapause embryos of *Artemia franciscana* (Kellogg). *Arch. Hydrobiol.* **52**, 415–439.
4. Clegg, J.S. (1997) Embryos of *Artemia franciscana* survive four years of continuous anoxia: the case for complete metabolic rate depression. *J. Exp. Biol.* **200**, 467–475.
5. Clegg, J.S., Jackson, S.A. & Popov, V.I. (2000) Long-term anoxia in encysted embryos of the crustacean, *Artemia franciscana*: viability, ultrastructure, and stress proteins. *Cell Tissue Res.* **301**, 433–444.
6. Clegg, J.S., Willsie, J.K. & Jackson, S.A. (1999) Adaptive significance of a small heatshock/α-crystallin protein (p26) in encysted embryos of the brine shrimp, *Artemia franciscana*. *Am. Zool.* **39**, 836–847.
7. Drinkwater, L.E. & Clegg, J.S. (1991) Experimental biology of cyst diapause. In *Artemia Biology* (Browne, R.A., Sorgeloos, P. & Trotman, C.N.A., eds), pp. 93–117. CRC Press, Inc., Boca Raton, FL.
8. Liang, P. & MacRae, T.H. (1999) The synthesis of a small heat shock/α-crystallin protein in *Artemia and* its relationship to stress tolerance during development. *Dev. Biol.* **207**, 445–456.
9. Jackson, S.A. & Clegg, J.S. (1996) Ontogeny of low molecular weight stress protein p26 during early development of the brine shrimp, *Artemia franciscana*. *Dev. Growth Differ.* **38**, 153–160.
10. Crack, J.A., Mansour, M., Sun, Y. & MacRae, T.H. (2002) Functional analysis of a small heat shock/α-crystallin protein from *Artemia franciscana*: oligomerization and thermotolerance. *Eur. J. Biochem.* **269**, 933–942.
11. Viner, R.I. & Clegg, J.S. (2001) Influence of trehalose on the molecular chaperone activity of p26, a small heat shock/α-crystallin protein. *Cell Stress Chaperones* **6**, 126–135.
12. Liang, P., Amons, R., MacRae, T.H. & Clegg, J.S. (1997) Purification, structure and *in vitro* molecular-chaperone activity of *Artemia* p26, a small heat-shock/α-crystallin protein. *Eur. J. Biochem.* **243**, 225–232.
13. Liang, P., Amons, R., Clegg, J.S. & MacRae, T.H. (1997) Molecular characterization of a small heat shock/α-crystallin protein in encysted *Artemia* embryos. *J. Biol. Chem.* **272**, 19051–19058.
14. Clegg, J.S., Jackson, S.A. & Warner, A.H. (1994) Extensive intracellular translocations of a major protein accompany anoxia in embryos of *Artemia franciscana*. *Exp. Cell Res.* **212**, 77–83.
15. Narberhaus, F. (2002) α-Crystallin-type heat shock proteins: socializing minichaperones in the context of a multichaperone network. *Microbiol. Mol. Biol. Rev.* **66**, 64–93.
16. MacRae, T.H. (2000) Structure and function of small heat shock/α-crystallin proteins: established concepts and emerging ideas. *Cell. Mol. Life Sci.* **57**, 899–913.
17. Slobin, L.I. (1980) Eukaryotic elongation factor T and artemin: two antigenically related proteins which reflect the dormant state of *Artemia* cysts. In *The Brine Shrimp, Artemia* (Persoone, G., Sorgeloos, P., Roels, O. & Jaspers, E., eds), Vol. 2, pp. 557–573. Universa Press, Wetteren, Belgium.
18. Baloh, R.H., Tansey, M.G., Lampe, P.A., Fahrner, T.J., Enomoto, H., Simburger, K.S., Leitner, M.L., Araki, T., Johnson, E.M. Jr & Milbrandt, J. (1998) Artemin, a novel member of the GDNF ligand family, supports peripheral and central neurons and signals through the GRFα3-RET receptor complex. *Neuron* **21**, 1291–1302.
19. De Herdt, E., Slegers, H. & Kondo, M. (1979) Identification and characterization of a 19-S complex containing a 27 000-M_r protein in *Artemia salina*. *Eur. J. Biochem.* **96**, 423–430.
20. De Herdt, E., Slegers, H. & Kondo, M. (1980) The 27 000-M_r protein of the 19 S cytoplasmic complex of *Artemia* is one of the major RNA-binding proteins. In *The Brine Shrimp, Artemia* (Persoone, G., Sorgeloos, P., Roels, O. & Jaspers, E., eds), Vol, 2, pp. 395–412. Universa Press, Wetteren, Belgium.
21. De Herdt, E., De Voeght, F., Clauwaert, J., Kondo, M. & Slegers, H. (1981) A cryptobiosis-specific 19S protein complex of *Artemia salina* gastrulae. *Biochem. J.* **194**, 9–17.
22. Möller, W., Amons, R., Janssen, G., Lenstra, J.A. & Maassen, J.A. (1987) Studies on elongation factor 1 and ribosomes of *Artemia*. In *Artemia Research and its Applications* (Decleir, W., Moens, L., Slegers, H., Jaspers, E. & Sorgeloos, P., eds), Vol. 2, pp. 451–469. Universa Press, Wetteren, Belgium.
23. De Graaf, J., Amons, R. & Möller, W. (1990) The primary structure of artemin from *Artemia* cysts. *Eur. J. Biochem.* **193**, 737–750.
24. Crichton, R.R. (1990) Proteins of iron storage and transport. *Adv. Protein Chem.* **40**, 281–363.
25. Theil, E.C. (1990) The ferritin family of iron storage proteins. *Adv. Enzymol. Relat. Areas Mol. Biol.* **63**, 421–449.

26. Harrison, P.M. & Arosio, P. (1996) The ferritins: molecular properties, iron storage function and cellular regulation. *Biochim. Biophys. Acta* **1275**, 161–203.
27. Hempstead, P.D., Yewdall, S.J., Fernie, A.R., Lawson, D.M., Artymiuk, P.J., Rice, D.W., Ford, G.C. & Harrison, P.M. (1997) Comparison of the three-dimensional structures of recombinant human H and horse L ferritins at high resolution. *J. Mol. Biol.* **268**, 424–448.
28. Charlesworth, A., Georgieva, T., Gospodov, I., Law, J.H., Dunkov, B.C., Ralcheva, N., Barillas-Mury, C., Ralchev, K. & Kafatos, F.C. (1997) Isolation and properties of *Drosophila melanogaster* ferritin: molecular cloning of a cDNA that encodes one subunit, and localization of the gene on the third chromosome. *Eur. J. Biochem.* **247**, 470–475.
29. Georgieva, T., Dunkov, B.C., Dimov, S., Ralchev, K. & Law, J.H. (2002) *Drosophila melanogaster* ferritin: cDNA encoding a light chain homologue, temporal and tissue specific expression of both subunit types. *Insect. Biochem. Mol. Biol.* **32**, 295–302.
30. Grossman, M.J., Hinton, S.M., Minak-Bernero, V., Slaughter, C. & Stiefel, E.I. (1992) Unification of the ferritin family of proteins. *Proc. Natl Acad. Sci. USA* **89**, 2419–2423.
31. Petit, J.-M., Briat, J.-F. & Lobréaux, S. (2001) Structure and differential expression of the four members of the *Arabidopsis thaliana* ferritin gene family. *Biochem. J.* **359**, 575–582.
32. Truty, J., Malpe, R. & Linder, M.C. (2001) Iron prevents ferritin turnover in hepatic cells. *J. Biol. Chem.* **276**, 48775–48780.
33. Langdon, C.M., Bagshaw, J.C. & MacRae, T.H. (1990) Tubulin isoforms in the brine shrimp, *Artemia*: prmary gene products and their posttranslational modification. *Eur. J. Cell Biol.* **52**, 217–226.
34. Rafiee, P., Matthews, C.O., Bagshaw, J.C. & MacRae, T.H. (1986) Reversible arrest of *Artemia* development by cadmium. *Can. J. Zool.* **64**, 1633–1641.
35. Go, E.C., Pandey, A.S. & MacRae, T.H. (1990) Effect of inorganic mercury on the emergence and hatching of the brine shrimp, *Artemia franciscana*. *Mar. Biol.* **107**, 93–102.
36. Langdon, C.M., Freeman, J.A. & MacRae, T.H. (1991) Post-translationally modified tubulins in *Artemia*: Prelarval development in the absence of detyrosinated tubulin. *Dev. Biol.* **148**, 2147–2155.
37. Chen, Q., Neville, C., MacKenzie, A. & Korneluk, R. (1996) Automated DNA sequencing requiring no DNA template purification. *Biotechniques* **21**, 453–457.
38. Marck, C. (1992) *DNA strider, version 1.2*. Service de Biochimie-Bat 142, Centre d'Etudes Nucléaires de Saclay, Gif-Sur-Yvette.
39. Neininger, A., Kontoyiannis, D., Kotlyarov, A., Winzen, R., Eckert, R., Volk, H.-D., Holtmann, H., Kollias, G. & Gaestel, M. (2002) MK2 targets AU-rich elements and regulates biosynthesis of tumor necrosis factor and interlukin-6 independently at different post-transcriptional levels. *J. Biol. Chem.* **277**, 3065–3068.
40. Sessler, A.M., Kaur, N., Palta, J.P. & Ntambi, J.M. (1996) Regulation of stearoyl-CoA desaturase 1 mRNA stability by polyunsaturated fatty acids in 3T3-L1 adipocytes. *J. Biol. Chem.* **271**, 29854–29858.
41. Chen, C.-Y.A. & Shyu, A.-B. (1995) AU rich elements: characterization and importance in mRNA degradation. *Trends Biochem. Sci.* **20**, 465–470.
42. Han, J., Brown, T. & Beutler, B. (1990) Endotoxin-responsive sequences control cachectin/tumor necrosis factor biosynthesis at the translational level. *J. Exp. Med.* **171**, 465–475.
43. Kruys, V., Marinx, O., Shaw, G., Deschamps, J. & Huez, G. (1989) Translational blockade imposed by cytokine-derived UA-rich sequences. *Science* **245**, 852–855.
44. Shaw, G. & Kamen, R. (1986) A conserved AU sequence from the 3′ untranslated region of GM-CSF mRNA mediates selective mRNA degradation. *Cell* **46**, 659–667.
45. Thiede, M.A. & Strittmatter, P. (1985) The induction and characterization of rat liver stearyl-CoA desaturase mRNA. *J. Biol. Chem.* **260**, 14459–14463.
46. Padgett, R.A., Grabowski, P.J., Konarska, M.M., Seiler, S. & Sharp, P.A. (1986) Splicing of messenger RNA precursors. *Annu. Rev. Biochem.* **55**, 1119–1150.
47. Kaestner, K.H., Ntambi, J.M., Kelly, T.J. Jr & Lane, M.D. (1989) Differentiation-induced gene expression in 3T3-L1 preadipocytes. A second differentially expressed gene encoding stearoyl-CoA desaturase. *J. Biol. Chem.* **264**, 14755–14761.
48. Vakalopoulou, E., Schaack, J. & Shenk, T. (1991) A 32-kilodalton protein binds to AU-rich domains in the 3′-untranslated regions of rapidly degraded mRNAs. *Mol. Cell. Biol.* **11**, 3355–3364.
49. Jackson, R.J. (1993) Cytoplasmic regulation of mRNA function: the importance of the 3′untranslated region. *Cell* **74**, 9–14.
50. Zhang, L., Ge, L., Parimoo, S., Stenn, K. & Prouty, S.M. (1999) Human stearoyl-CoA desaturase: alternative transcripts generated from a single gene by usage of tandem polyadenylation sites. *Biochem. J.* **340**, 255–264.
51. Willsie, J.K. & Clegg, J.S. (2002) Small heat shock protein p26 associates with nuclear lamins and HSP70 in nuclei and nuclear matrix fractions from stressed cells. *J. Cell. Biochem.* **84**, 601–614.
52. Kim, S.-J., Jeong, D.-G., Chi, S.-W., Lee, J.-S. & Ryu, S.-E. (2001) Crystal structure of proteolytic fragments of the redox-sensitive Hsp33 with constitutive chaperone activity. *Nat. Struct. Biol.* **8**, 459–466.
53. Barbirz, S., Jakob, U. & Glocker, M.O. (2000) Mass spectrometry unravels disulfide bond formation as the mechanism that activates a molecular chaperone. *J. Biol. Chem.* **275**, 18759–18766.
54. Landino, L.M., Hasan, R., McGaw, A., Cooley, S., Smith, A.W., Masselam, K. & Kim, G. (2002) Peroxynitrite oxidation of tubulin sulfhydryls inhibits microtubule polymerization. *Arch. Biochem. Biophys.* **398**, 213–220.
55. Manalo, D.J., Lin, Z. & Liu, A.Y.-C. (2002) Redox-dependent regulation of the conformation and function of human heat shock factor 1. *Biochemistry* **41**, 2580–2588.
56. Kakhlon, O., Gruenbaum, Y., Cabantchik, Z. (2002) Ferritin expression modulates cell cycle dynamics and cell responsiveness to H-ras-induced growth via expansion of the labile iron pool. *Biochem. J.* **363**, 431–436.